Electric Power Systems Research 84 (2012) 135–143

Contents lists available at SciVerse ScienceDirect

Electric Power Systems Research

journal homepage: www.elsevier.com/locate/epsr

Observer-based nonlinear control of power system using sliding mode control strategy

M. Ouassaid [a,*], M. Maaroufi [b], M. Cherkaoui [b]

[a] Department of Industrial Engineering, Caddi AAyad University, Ecole Nationale des Sciences Appliquées, B.P. 63, Sidi Bouzid, Safi, Morocco
[b] Department of Electrical Engineering, Mohammed V University, Ecole Mohammadia d'Ingénieurs, B.P. 765, Agdal, Rabat, Morocco

ARTICLE INFO

Article history:
Received 13 November 2009
Received in revised form 27 February 2011
Accepted 28 October 2011
Available online 25 November 2011

Keywords:
Sliding mode control
Lyapunov methods
Damper currents observer
Power system
Transient stability

ABSTRACT

This paper presents a new transient stabilization with voltage regulation analysis approach of a synchronous power generator driven by steam turbine and connected to an infinite bus. The aim is to obtain high performance for the terminal voltage and the rotor speed simultaneously under a large sudden fault and a wide range of operating conditions. The methodology adopted is based on sliding mode control technique. First, a nonlinear sliding mode observer for the synchronous machine damper currents is constructed. Second, the stabilizing feedback laws for the complete ninth order model of a power system, which takes into account the stator dynamics as well as the damper effects, are developed. They are shown to be asymptotically stable in the context of Lyapunov theory. Simulation results, for a single-Machine-Infinite-Bus (SMIB) power system, are given to demonstrate the effectiveness of the proposed combined observer–controller for the transient stabilization and voltage regulation.

1. Introduction

Successful operation of power system depends largely on the ability to provide reliable and uninterrupted service. The reliability of the power supply implies much more than merely being available. Ideally, the loads must be fed at constant voltage and frequency at all times. However, small or large disturbances such as power changes or short circuits may transpire. One of the most vital operation demands is maintaining good stability and transient performance of the terminal voltage, rotor speed and the power transfer to the network [1,2]. This requirement should be achieved by an adequate control of the system.

The high complexity and nonlinearity of power systems, together with their almost continuously time varying nature, require candidate controllers to be able to take into account the important nonlinearities of the power system model and to be independent of the equilibrium point. Much attention has been given to the application of nonlinear control techniques to solve the transient stabilization problem [3,4]. Most of these controllers are based on feedback linearization technique [5–9]. The main objective in these works was to enhance the system stability and damping performance through excitation control. The nonlinear model used in these studies was a reduced third order model of the synchronous machine. In Ref. [10], the feedback linearization technique was used to control the rotor angle as well as the terminal voltage, using the excitation and the turbine's servo-motor input. It is based on a 7th order model of the synchronous machine. Feedback linearization is recently enhanced by using robust control designs such as H_∞ control and L_2 disturbance attenuation [11,12]. Several modern control approaches including methods based on the passivity principle [13,14], fuzzy logic and neural networks [15,16], backstepping design [17,18], have been used to design continuous nonlinear control algorithms which overcome the known limitations of traditional linear controllers: Automatic Voltage Regulator (AVR) and the Power System Stabilizer (PSS) [19–22].

New modern control techniques will continue to fascinate researchers looking for further improvements in high performance power system stability. The sliding mode control approach has been recognized as one of the efficient tools to design robust controllers for complex high-order nonlinear dynamic plants operating under various uncertainty conditions. The major advantage of sliding mode is the low sensitivity to plant parameter variations and disturbances which relaxes the necessity of exact modelling [23].

In this paper, a sliding mode controller has been constructed based on a time-varying sliding surface to control the rotor speed and terminal voltage, simultaneously, in order to enhance the transient stability and to ensure good post-fault voltage regulation for power system. It is based on a detailed 9th order model of a system which consists of a steam turbine and SMIB and takes into account the stator dynamics as well as the damper winding effects and practical limitation on controls. However damper currents are not available for measurement. Consequently, an observer of damper currents is proposed.

* Corresponding author. Tel.: +21 2678 03 50 59; fax: +21 2524 66 80 12.
E-mail addresses: ouassaid@yahoo.fr, ouassaid@emi.ac.ma (M. Ouassaid).

0378-7796/$ – see front matter © 2011 Elsevier B.V. All rights reserved.
doi:10.1016/j.epsr.2011.10.014

The rest of this paper is organized as follows. In Section 2, the dynamic equations of the system under study are presented. A new nonlinear observer for damper winding currents is developed in Section 3. In Section 4, the nonlinear excitation voltage and rotor speed controllers are derived. Section 5 deals with a number of numerical simulations results of the proposed observer-based nonlinear controller. Finally, conclusions are mentioned in Section 6.

2. Mathematical model of power system studied

The system to be controlled, studied in this work, is shown in Fig. 1. It consists of synchronous generator driven by steam turbine and connected to an infinite bus via a transmission line. The synchronous generator is described by a 7th order nonlinear mathematical model which comprises three stator windings, one field winding and two damper windings. The mathematical model of the plant, which is presented in some details in [10,24] can be written as follows:

Electrical equations:

$$\dot{x}_1 = a_{11}x_1 + a_{12}x_2 + a_{13}x_3x_6 + a_{14}x_4 + a_{15}x_6x_5 + a_{16}\cos(-x_7+\sigma) + b_1u_{fd} \quad (1)$$

$$\dot{x}_2 = a_{21}x_1 + a_{22}x_2 + a_{23}x_3x_6 + a_{24}x_4 + a_{25}x_6x_5 + a_{26}\cos(-x_7+\sigma) + b_2u_{fd} \quad (2)$$

$$\dot{x}_3 = a_{31}x_1x_6 + a_{32}x_2x_6 + a_{33}x_3 + a_{34}x_4x_6 + a_{35}x_5 + a_{36}\sin(-x_7+\sigma) \quad (3)$$

$$\dot{x}_4 = a_{41}x_1 + a_{42}x_2 + a_{43}x_3x_6 + a_{44}x_4 + a_{45}x_6x_5 + a_{46}\cos(-x_7+\sigma) + b_3u_{fd} \quad (4)$$

$$\dot{x}_5 = a_{51}x_1x_6 + a_{52}x_2x_6 + a_{53}x_3 + a_{54}x_4x_6 + a_{55}x_5 + a_{56}\sin(-x_7+\sigma) \quad (5)$$

Mechanical equations:

$$\dot{x}_6 = a_{61}x_6 + a_{62}\left(\frac{x_8}{x_6}\right) - a_{62}T_e \quad (6)$$

$$\dot{x}_7 = \omega_R(x_6 - 1) \quad (7)$$

Turbine dynamics [25]:

$$\dot{x}_8 = a_{81}x_8 + a_{82}x_9 \quad (8)$$

Turbine valve control [25]:

$$\dot{x}_9 = a_{91}x_9 + a_{92}x_6 + b_4u_g \quad (9)$$

where $x = [i_d, i_{fd}, i_q, i_{kd}, i_{kq}, \omega, \delta, P_m, X_e]^T$ is the vector of state variables, u_{fd} the excitation control input, u_g the input power of control system. The parameters a_{ij} and b_i are described in Appendix A.

The machine terminal voltage is calculated from Park components v_d and v_q as follows [10,24]:

$$v_t = (v_d^2 + v_q^2)^{1/2} \quad (10)$$

with

$$v_d = c_{11}x_1 + c_{12}x_2 + c_{13}x_3x_6 + c_{14}x_4 + c_{15}x_5x_6 + c_{16}\cos(-x_7+\sigma) + c_{17}u_{fd} \quad (11)$$

$$v_q = c_{21}x_1x_6 + c_{22}x_2x_6 + c_{23}x_3 + c_{24}x_4x_6 + c_{25}x_5 + c_{26}\sin(-x_7+\sigma) \quad (12)$$

where c_{ij} are coefficients which depend on the coefficients a_{ij}, on the infinite bus phase voltage V^∞ and the transmission line parameters R_e and L_e. They are described in Appendix A.

Available states for synchronous generator are the stator phase currents i_d and i_q, voltages at the terminals of the machine v_d and v_q, field current i_{fd}. It is also assumed that the angular speed ω and the power angle δ are available for measurement [26]. In the next section the development of an observer of the damper currents i_{kd} and i_{kq} will be presented.

3. Development of a sliding mode observer for the damper winding currents

For continuous time systems, the state space representation of the electrical dynamics of the power system model (1)–(5) is:

$$\frac{d}{dt}\begin{bmatrix}x_1\\x_2\\x_3\end{bmatrix} = F_{11}\begin{bmatrix}x_1\\x_2\\x_3\end{bmatrix} + F_{12}\begin{bmatrix}x_4\\x_5\end{bmatrix} + \begin{bmatrix}b_1\\b_2\\0\end{bmatrix}u_{fd} + H_1(t) \quad (13)$$

$$\frac{d}{dt}\begin{bmatrix}x_4\\x_5\end{bmatrix} = F_{21}\begin{bmatrix}x_1\\x_2\\x_3\end{bmatrix} + F_{22}\begin{bmatrix}x_4\\x_5\end{bmatrix} + \begin{bmatrix}b_3\\0\end{bmatrix}u_{fd} + H_2(t) \quad (14)$$

where

$$H_1(t) = [a_{16}\cos(-x_7+\sigma), a_{26}\cos(-x_7+\sigma), a_{36}\sin(-x_7+\sigma)]^T,$$

$$H_2(t) = [a_{46}\cos(-x_7+\sigma), a_{56}\sin(-x_7+\sigma)]^T$$

$$F_{11} = \begin{bmatrix}a_{11} & a_{12} & a_{13}x_6\\ a_{21} & a_{22} & a_{23}x_6\\ a_{31}x_6 & a_{32}x_6 & a_{33}\end{bmatrix}, \quad F_{21} = \begin{bmatrix}a_{41} & a_{42} & a_{43}x_6\\ a_{51}x_6 & a_{52}x_6 & a_{53}\end{bmatrix},$$

$$F_{12} = \begin{bmatrix}a_{14} & a_{15}x_6\\ a_{24} & a_{25}x_6\\ a_{34}x_6 & a_{35}\end{bmatrix}, \quad F_{22} = \begin{bmatrix}a_{44} & a_{45}x_6\\ a_{54}x_6 & a_{55}\end{bmatrix}$$

To construct the sliding mode observer, let define the switching surface S as follows:

$$S(t) = \begin{bmatrix}\hat{x}_1 - x_1\\ \hat{x}_2 - x_2\\ \hat{x}_3 - x_3\end{bmatrix} \equiv \begin{bmatrix}e_1\\e_2\\e_3\end{bmatrix} = 0 \quad (15)$$

Then, an observer for (13) is constructed as:

$$\frac{d}{dt}\begin{bmatrix}\hat{x}_1\\\hat{x}_2\\\hat{x}_3\end{bmatrix} = F_{11}\begin{bmatrix}\hat{x}_1\\\hat{x}_2\\\hat{x}_3\end{bmatrix} + F_{12}\begin{bmatrix}\hat{x}_4\\\hat{x}_5\end{bmatrix} + \begin{bmatrix}b_1\\b_2\\0\end{bmatrix}u_{fd} + H_1(t) + K\begin{bmatrix}\mathrm{sgn}(\hat{x}_1 - x_1)\\ \mathrm{sgn}(\hat{x}_2 - x_2)\\ \mathrm{sgn}(\hat{x}_3 - x_3)\end{bmatrix} \quad (16)$$

where $\hat{x}_1, \hat{x}_2$ and $\hat{x}_3$ are the observed values of i_d, i_{fd} and i_q, K is the switching gain, and sgn is the sign function. Moreover, the damper current observer is given from (14) as:

$$\frac{d}{dt}\begin{bmatrix}\hat{x}_4\\\hat{x}_5\end{bmatrix} = F_{21}\begin{bmatrix}\hat{x}_1\\\hat{x}_2\\\hat{x}_3\end{bmatrix} + F_{22}\begin{bmatrix}\hat{x}_4\\\hat{x}_5\end{bmatrix} + \begin{bmatrix}b_3\\0\end{bmatrix}u_{fd} + H_2(t) \quad (17)$$

where $\hat{x}_4$ and $\hat{x}_5$ are the observed values of i_{kd} and i_{kq}.

Subtracting (13) from (16), the error dynamics can be written:

$$\frac{d}{dt}\begin{bmatrix}e_1\\e_2\\e_3\end{bmatrix} = F_{11}\begin{bmatrix}e_1\\e_2\\e_3\end{bmatrix} + F_{12}\begin{bmatrix}\tilde{x}_4\\\tilde{x}_5\end{bmatrix} + K\begin{bmatrix}sgn\, e_1\\ sgn\, e_2\\ sgn\, e_3\end{bmatrix} \quad (18)$$

where $\tilde{x}_4$ and $\tilde{x}_5$ are the estimation errors of the damper currents x_4 and x_5.

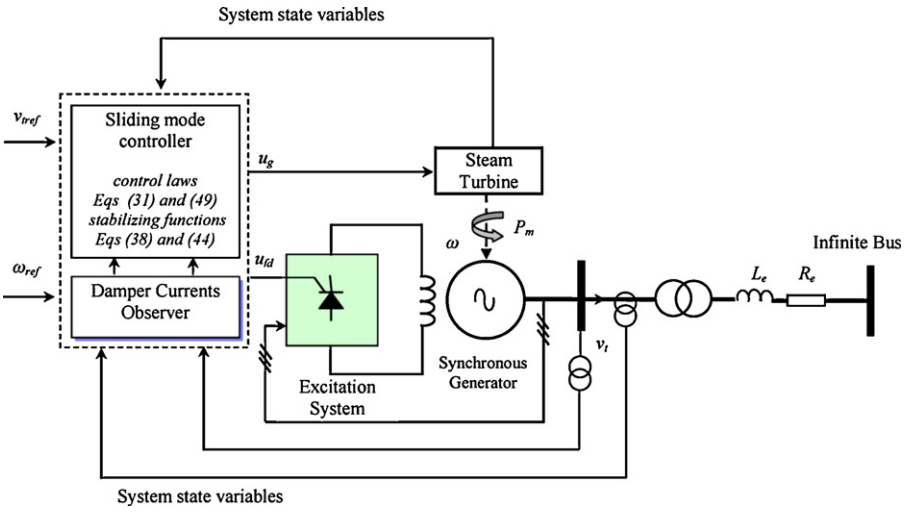

Fig. 1. Control system configuration.

The switching gain is designed as:

$$K = \min \times \left\{ \begin{array}{l} -a_{11}|e_1| - (a_{12}e_2 + a_{13}\omega e_3 + a_{14}\tilde{x}_4 + a_{15}\omega\tilde{x}_5)sgn\, e_1 \\ -a_{22}\,|e_2| - (a_{21}e_1 + a_{23}\omega e_3 + a_{24}\tilde{x}_4 + a_{25}\omega\tilde{x}_5)\,sgn\, e_2 \\ -a_{33}\,|e_3| - (a_{31}\omega e_1 + a_{32}\omega e_2 + a_{34}\omega\tilde{x}_4 + a_{35}\tilde{x}_5)\,sgn\, e_3 \end{array} \right\} - \xi \tag{19}$$

where ξ is a positive small value.

Theorem 1. *The globally asymptotic stability of (18) is guaranteed, if the switching gain is given by (19).*

Proof. The stability of the overall structure is guaranteed through the stability of the direct axis and quadrature axis currents x_1, x_2, and field current x_3 observer. The Lyapunov function for the proposed sliding mode damper current is chosen as:

$$V_{obs} = \frac{1}{2}S^T \Gamma S \tag{20}$$

where Γ is an identity positive matrix.

Therefore, the derivative of the Lyapunov function is

$$\dot{V}_{obs} = S^T \Gamma \dot{S} = \begin{bmatrix} e_1 \\ e_2 \\ e_3 \end{bmatrix}^T \Gamma \left(F_{11} \begin{bmatrix} e_1 \\ e_2 \\ e_3 \end{bmatrix} + F_{12} \begin{bmatrix} \tilde{x}_4 \\ \tilde{x}_5 \end{bmatrix} + K \begin{bmatrix} sgn\, e_1 \\ sgn\, e_2 \\ sgn\, e_3 \end{bmatrix} \right) = G_1 + G_2 + G_3 \tag{21}$$

where

$$G_1 = a_{11}e_1^2 + a_{12}e_1e_2 + a_{13}\omega e_1e_3 + a_{14}e_1\tilde{x}_4 + a_{15}\omega e_1\tilde{x}_5 + K|e_1|$$
$$G_2 = a_{21}e_1e_2 + a_{22}e_2^2 + a_{23}\omega e_2e_3 + a_{24}e_2\tilde{x}_4 + a_{25}\omega e_2\tilde{x}_5 + K|e_2|$$
$$G_3 = a_{31}\omega e_1e_3 + a_{32}\omega e_2e_3 + a_{33}e_3^2 + a_{34}\omega e_3\tilde{x}_4 + a_{35}e_3\tilde{x}_5 + K|e_3|$$

Using the designed switching gain in (19), both G_1, G_2 and G_3 are negatives. Therefore, $\dot{V}_{obs}$ is a negative definite, and the sliding mode condition is satisfied [27]. Furthermore the global asymptotic stability of the observer is guaranteed.

According to (19) by a proper selection of ξ, the influence of parametric uncertainties of the SMIB can be much reduced.

The switching gain must large enough to satisfy the reaching condition of sliding mode. Hence the estimation error is confined into the sliding hyerplane:

$$\frac{d}{dt}\begin{bmatrix} e_1 \\ e_2 \\ e_3 \end{bmatrix} = \begin{bmatrix} e_1 \\ e_2 \\ e_3 \end{bmatrix} = 0 \tag{22}$$

However, if the switching gain is too large, the chattering noise may lead to estimation errors. To avoid the chattering phenomena, the sign function is replaced by the following continuous function in simulation:

$$\frac{S(t)}{|S(t)| + \varsigma_1}$$

where ς_1 is a positive constant. □

4. Design of sliding mode terminal voltage and speed controller

4.1. Terminal voltage control law

The dynamic of the terminal voltage (23), is obtained through the time derivative of (10) using (11) and (12) where the damper currents are replaced by the observer (17):

$$\frac{dv_t}{dt} = \frac{1}{v_t}\left(v_d\frac{dv_d}{dt} + v_q\frac{dv_q}{dt}\right) = \frac{v_q}{v_t}\frac{dv_q}{dt} + c_{17}\frac{v_d}{v_t}\frac{du_{fd}}{dt} + \frac{v_d}{v_t}\left[c_{11}\frac{dx_1}{dt} + c_{12}\frac{dx_2}{dt} + c_{13}x_6\frac{dx_3}{dt} + c_{13}x_3\frac{dx_6}{dt} + c_{14}\frac{d\hat{x}_4}{dt} + c_{15}x_6\frac{d\hat{x}_5}{dt} + c_{15}\hat{x}_5\frac{dx_6}{dt} + c_{16}\frac{dx_7}{dt}\sin(-x_7 + \sigma)\right] = c_{17}\frac{v_d}{v_t}\frac{du_{fd}}{dt} + f(x) \tag{23}$$

where

$$f(x) = \frac{v_q}{v_t}\frac{dv_q}{dt} + \frac{v_d}{v_t}\left[c_{11}\frac{dx_1}{dt} + c_{12}\frac{dx_2}{dt} + c_{13}x_6\frac{dx_3}{dt} + c_{13}x_3\frac{dx_6}{dt} + c_{14}\frac{d\hat{x}_4}{dt} + c_{15}\hat{x}_5\frac{dx_6}{dt} + c_{15}x_6\frac{d\hat{x}_5}{dt} + c_{16}\frac{dx_7}{dt}\sin(-x_7 + \sigma)\right]$$

Furthermore, we define the tracking error between terminal voltage and its reference as:

$$e_1 = v_t - v_t^{ref} \tag{24}$$

And its error dynamic is derived, using (23), as follows:

$$\frac{de_1}{dt} = c_{17}\frac{v_d}{v_t}\frac{du_{fd}}{dt} + f(x) \tag{25}$$

According to the (24), the proposed time-varying sliding surface is defined by:

$$S_1 = K_1 e_1(t) \tag{26}$$

where K_1 is a positive constant feedback gain. The next step is to design a control input which satisfies the sliding mode existence law. The control input is chosen to have the structure:

$$u(t) = u_{eq}(t) + u_n(t) \tag{27}$$

where $u_{eq}(t)$ is an equivalent control-input that determines the system's behavior on the sliding surface and $u_n(t)$ is a non-linear switching input, which drives the state to the sliding surface and maintains the state on the sliding surface in the presence of the parameter variations and disturbances. The equivalent control-input is obtained from the invariance condition and is given by the following condition [23] $S_1 = 0$ and $\dot{S}_1 = 0 \Rightarrow u(t) = u_{eq}(t)$

From the above equation:

$$\dot{S}_1 = K_1 c_{17} \frac{v_d}{v_t} \frac{du_{fd}}{dt} + K_1 f(x) = 0 \tag{28}$$

Therefore, the equivalent control-input is given as:

$$u_{eq}(t) = -\frac{v_t}{c_{17} v_d} f(x) \tag{29}$$

By choosing the nonlinear switching input $u_n(t)$ as follows:

$$u_n(t) = -\alpha_1 \frac{v_t}{c_{17} v_d} sgn(e_1) \tag{30}$$

where α_1 is a positive constant. The control input is given from (27), (29) and (30) as follows:

$$u(t) = \frac{du_{fd}}{dt} = -\frac{v_t}{c_{17} v_d}(f(x) + \alpha_1 sgn(e_1)) \tag{31}$$

Using the proposed control law (31), the reachability of sliding mode control of (25) is guaranteed.

4.2. Sliding mode rotor speed controller

We now focused our attention to the rotor speed tracking objective. The sliding mode-based rotor speed control methodology proposed consists of three steps:

Step 1: The rotor speed error is:

$$e_2 = x_6 - \omega^{ref} \tag{32}$$

where $\omega^{ref} = 1$ p.u. is the desired trajectory. The sliding surface is selected as:

$$S_2 = K_2 e_2(t) \tag{33}$$

where K_2 is a positive constant. From (32) and (6), the derivative of the sliding surface (33) can be given as:

$$\frac{dS_2}{dt} = K_2 \left(a_{61} x_6 + a_{62} \frac{x_8}{x_6} - a_{62} T_e \right) \tag{34}$$

The x_8 can be viewed as a virtual control in the above equation. To ensure the Lyapunov stability criteria i.e. $\dot{S}_2 S_2 \prec 0$ we define the nonlinear control input x^*_{8eq} as:

$$x^*_{8eq} = \frac{x_6}{a_{62}}(a_{62} T_e - a_{61} x_6) \tag{35}$$

The nonlinear switching input x^*_{8n} can be chosen as follows:

$$x^*_{8n} = -\alpha_2 \frac{x_6}{a_{62}} \text{sgn}(e_2) \tag{36}$$

where α_2 is a positive constant.

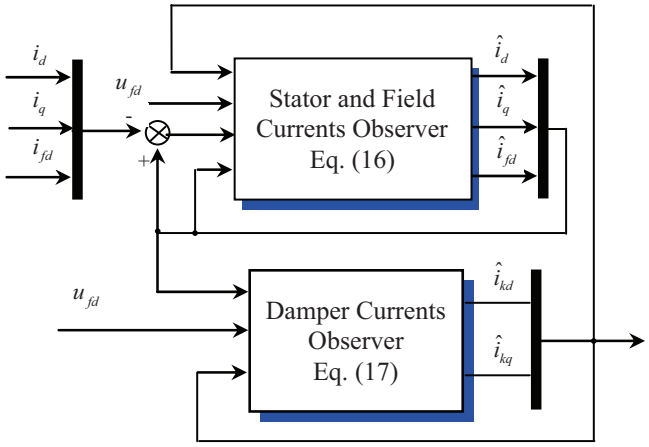

Fig. 2. Block diagram of the sliding mode damper currents observer.

Then, the stabilizing function of the mechanical power is obtained as:

$$x^*_8 = \frac{x_6}{a_{62}}(a_{62} T_e - a_{61} x_6 - \alpha_2 \text{sgn}(e_2)) \tag{37}$$

When a fault occurs, large currents and torques are produced. This electrical perturbation may destabilize the operating conditions. Hence, it becomes necessary to account for these uncertainties by designing a higher performance controller.

In (37), as electromagnetic load T_e is unknown, when fault occurs, it has to be estimated adaptively. Thus, let us define:

$$\hat{x}^*_8 = \frac{x_6}{a_{62}}(a_{62} \hat{T}_e - a_{61} x_6 - \alpha_2 \text{sgn}(e_2)) \tag{38}$$

where $\hat{T}_e$ is the estimated value of the electromagnetic load which should be determined later. Substituting (38) in (34), the rotor speed sliding surface dynamics becomes:

$$\frac{dS_2}{dt} = K_2(-\alpha_2 \text{sgn}(e_2) - a_{62} \tilde{T}_e) \tag{39}$$

where $\tilde{T}_e = T_e - \hat{T}_e$ is the estimation error of electromagnetic load.

Step 2: Since the mechanical power x_8 is not our control input, the stabilizing error between x_8 and its desired trajectory x^*_8 is defined as:

$$e_3 = x^*_8 - x_8 \tag{40}$$

To stabilize the mechanical power x_8, the sliding surface is selected as:

$$S_3 = K_3 e_3(t) \tag{41}$$

where K_3 is a positive constant. The derivative of S_3 using (40) and (8) is given as:

$$\frac{dS_3}{dt} = K_3 \left(a_{81} x_8 + a_{82} x_9 - \frac{dx^*_8}{dt} \right) \tag{42}$$

If we consider the steam valve opening x_9 as a second virtual control, the equivalent control x^*_{9eq} is obtained as the solution of the problem $\dot{S}_3(t) = 0$.

$$x^*_{9eq} = \frac{1}{a_{82}} \left(\frac{dx^*_8}{dt} - a_{81} x_8 \right) \tag{43}$$

Thus, the stabilizing function of the steam valve opening is obtained as:

$$x^*_9 = \frac{1}{a_{82}} \left(\frac{dx^*_8}{dt} - a_{81} x_8 - \alpha_3 \text{sgn}(e_3) \right) \tag{44}$$

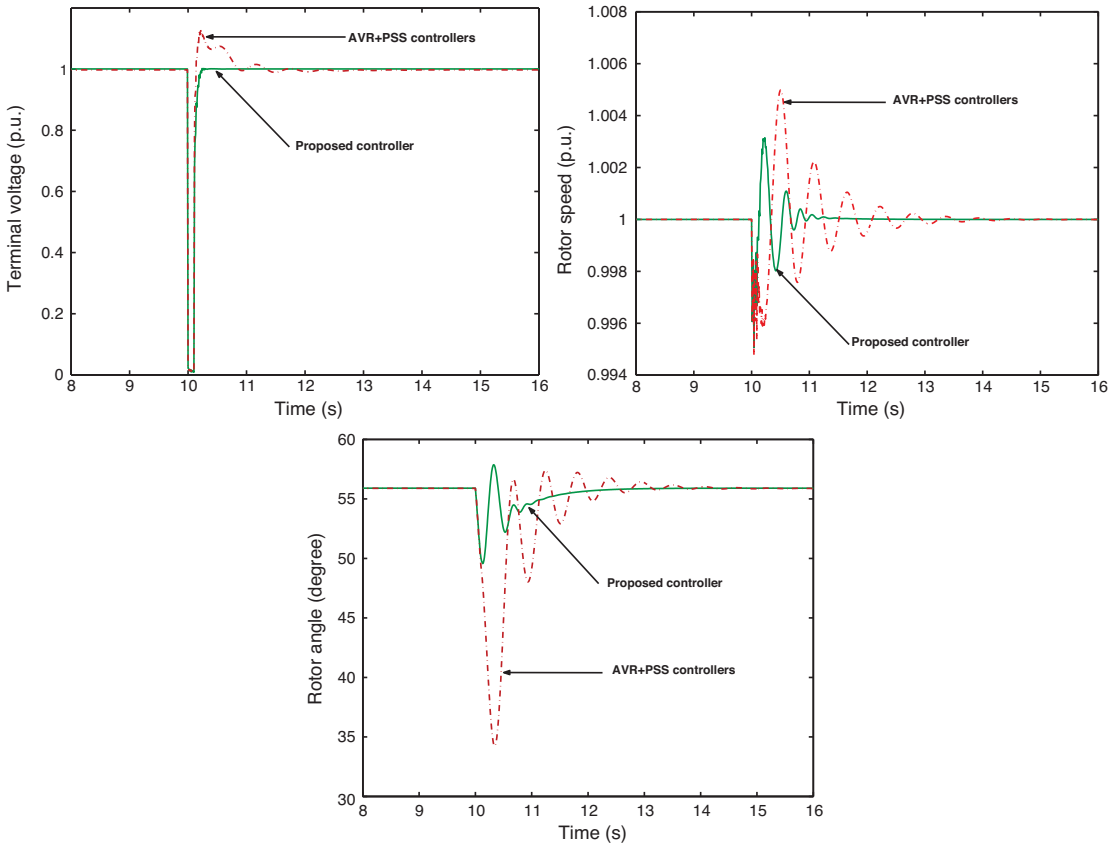

Fig. 3. Simulated result of the proposed controller under large sudden fault and operating point P_m = 0,6 p.u.

where α_3 is a positive constant. Substituting (44) in (42), the steam valve opening sliding surface dynamics becomes:

$$\frac{dS_3}{dt} = -\alpha_3 K_3 \,\mathrm{sgn}(e_3) \tag{45}$$

Step 3: In order to go one step ahead the steam valve opening error is defined as:

$$e_4 = x_9 - x_9^* \tag{46}$$

By defining a new sliding surface $S_4(t) = K_4 e_4(t)$ the derivative of S_4 is found by time differentiation of (46) and using (9):

$$\frac{dS_4}{dt} = K_4 \left(a_{91}x_9 + a_{92}x_6 + b_4 u_g - \frac{dx_9^*}{dt} \right) \tag{47}$$

To satisfy the reaching condition $\dot{S}_4 S_4 \prec 0$, the equivalent control $u_{geq}(t)$ is given as:

$$u_{geq} = \frac{1}{b_4}\left(\frac{dx_9^*}{dt} - a_{91}x_9 - a_{92}x_6 \right) \tag{48}$$

Next, the following choice of feedback control is made:

$$u_g = \frac{1}{b_4}\left(\frac{dx_9^*}{dt} - a_{91}x_9 - a_{92}x_6 - \alpha_4 \,\mathrm{sgn}(e_4) \right) \tag{49}$$

4.3. Stability analysis

Theorem 3. *The dynamic sliding mode control laws (31) and (49) with stabilizing functions (38) and (44) when applied to the single machine infinite power system, guarantee the asymptotic convergence of the outputs v_t and $x_6 = \omega$ to their desired values v_{tref} and $\omega_{ref} = 1$, respectively.*

Proof. Consider a positive definite Lyapunov function:

$$V_{con} = \frac{1}{2}S_1^2 + \frac{1}{2}S_2^2 + \frac{1}{2}S_3^2 + \frac{1}{2}S_4^2 + \frac{1}{2\mu}\tilde{T}_e^2 \tag{50}$$

Using (28), (39), (45) and (47), the derivative of (50) can be derived as follows:

$$\begin{aligned}\dot{V}_{con} = {} & \dot{S}_1 S_1 + \dot{S}_2 S_2 + \dot{S}_3 S_3 + \dot{S}_4 S_4 + \tilde{T}_e \frac{1}{\mu}\frac{d\tilde{T}_e}{dt} = K_1 c_{17}\frac{v_d}{v_t}\frac{du_{fd}}{dt} \\ & + K_1 f(x) + K_2(-\alpha_2 sgn(e_2) - a_{62}\tilde{T}_e) - \alpha_3 K_3 \,\mathrm{sgn}(e_3) \\ & + K_4\left(a_{91}x_9 + a_{92}x_6 + b_4 u_g - \frac{dx_9^*}{dt} \right) + \tilde{T}_e \frac{1}{\mu}\frac{d\tilde{T}_e}{dt}\end{aligned} \tag{51}$$

Substituting the control laws (31) and (49) in (51) produces:

$$\begin{aligned}\dot{V}_{con} = {} & -\alpha_1 K_1^2 e_1 \,\mathrm{sgn}(e_1) - \alpha_2 K_2^2 e_2 \,\mathrm{sgn}(e_2) - \alpha_3 K_3^2 e_3 \,\mathrm{sgn}(e_3) \\ & - \alpha_4 K_4^2 e_4 \,\mathrm{sgn}(e_3) - K_2^2 a_{62}\tilde{T}_e e_2 + \tilde{T}_e \frac{1}{\mu}\frac{d\tilde{T}_e}{dt} = -\alpha_1 K_1^2 |e_1| \\ & - \alpha_2 K_2^2 |e_2| - \alpha_3 K_3^2 |e_3| - \alpha_4 K_4^2 |e_4| + \left(\frac{1}{\mu}\frac{d\tilde{T}_e}{dt} - K_2^2 a_{62} e_2 \right)\tilde{T}_e\end{aligned} \tag{52}$$

To make the time derivative of V_{con} strictly negative, we choose the adaptive law as:

$$\frac{d\tilde{T}_e}{dt} = \mu a_{62} K_2^2 e_2 \tag{53}$$

Thus:

$$\begin{aligned}\dot{V}_{con} = {} & -\alpha_1 K_1^2 |e_1| - \alpha_2 K_2^2 |e_2| - \alpha_3 K_3^2 |e_3| \; - \alpha_4 K_4^2 |e_4| \\ = {} & -\sum_{i=1}^{4} \alpha_i K_i^2 |e_i| < 0\end{aligned} \tag{54}$$

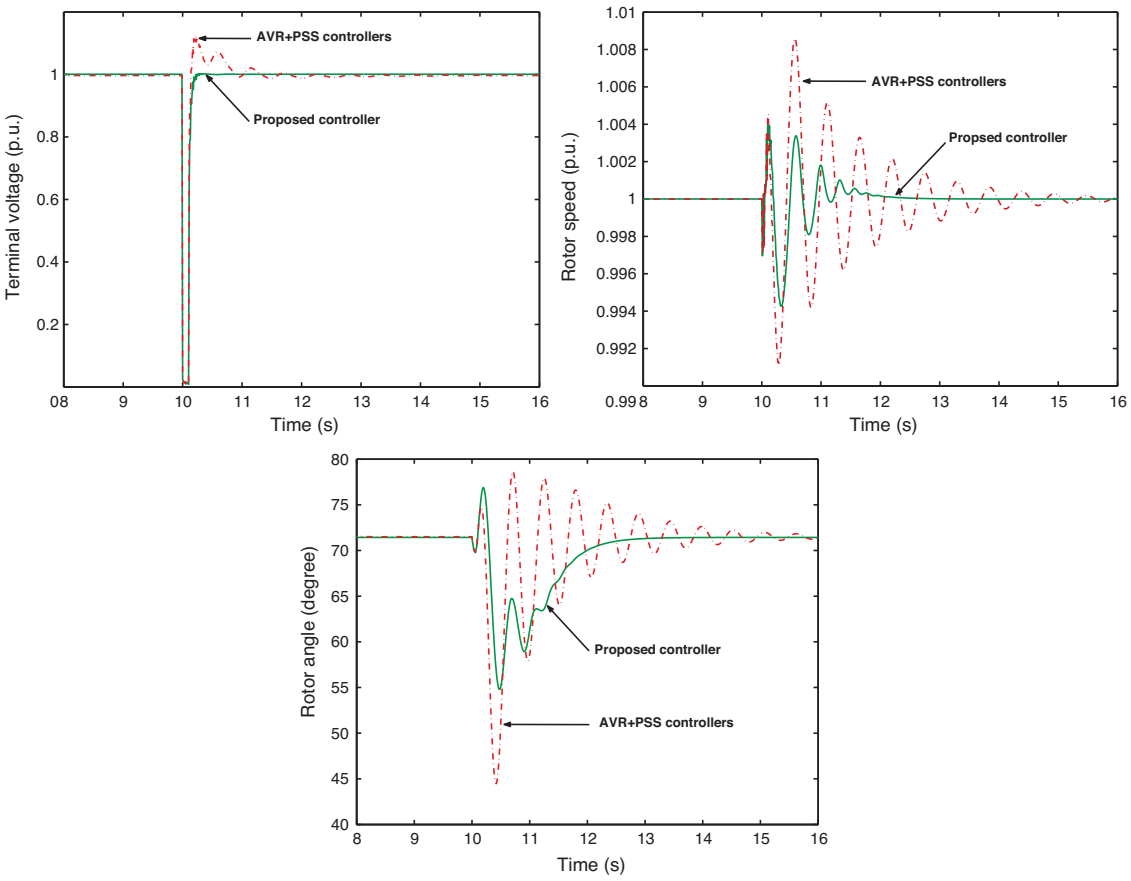

Fig. 4. Simulated result of the proposed controller under large sudden fault and operating point $P_m = 0{,}9$ p.u.

From the above analysis, it is evident that the reaching condition is guaranteed. □

Remark. In order to eliminate the chattering, the discontinuous control components in (31), (38), (44) and (49) can be replaced by a smooth sliding mode component to yield:

$$\frac{du_{fd}}{dt} = -\frac{v_t}{c_{17}v_d}\left(f(x) + \alpha_1 \frac{S_1(t)}{|S_1(t)| + \tau_2}\right)$$

$$x_8^* = \frac{x_6}{a_{62}}\left(a_{62}T_e - a_{61}x_6 - \alpha_2 \frac{S_2(t)}{|S_2(t)| + \tau_3}\right)$$

$$x_9^* = \frac{1}{a_{82}}\left(\frac{dx_8^*}{dt} - a_{81}x_8 - \alpha_3 \frac{S_3(t)}{|S_3(t)| + \tau_4}\right)$$

$$u_g = \frac{1}{b_4}\left(\frac{dx_9^*}{dt} - a_{91}x_9 - a_{92}x_6 - \alpha_4 \frac{S_4(t)}{|S_4(t)| + \tau_5}\right)$$

where $\tau_i \succ 0$ is a small constant. This modification creates a small boundary layer around the switching surface in which the system trajectory remains. Therefore, the chattering problem can be reduced significantly [23].

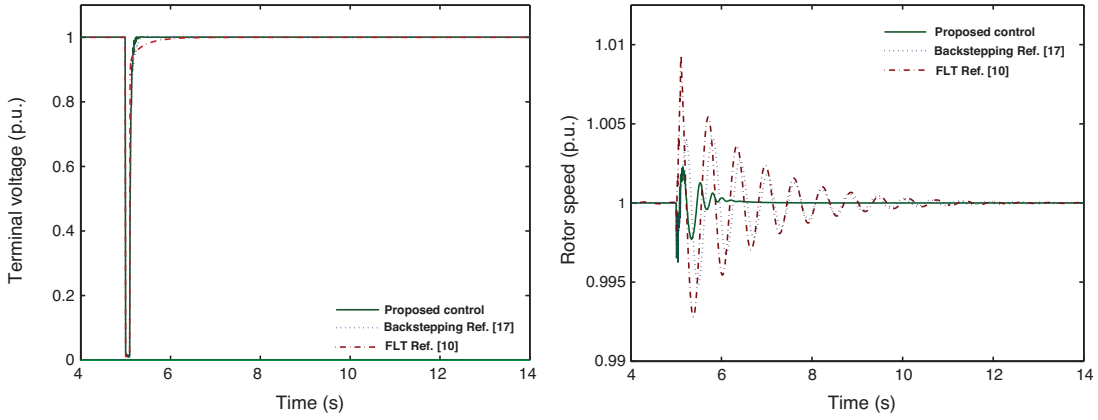

Fig. 5. Tracking performance comparison of the proposed observer based controller and nonlinear controllers (backstepping Ref. [17] and feedback linearization technique Ref. [10]).

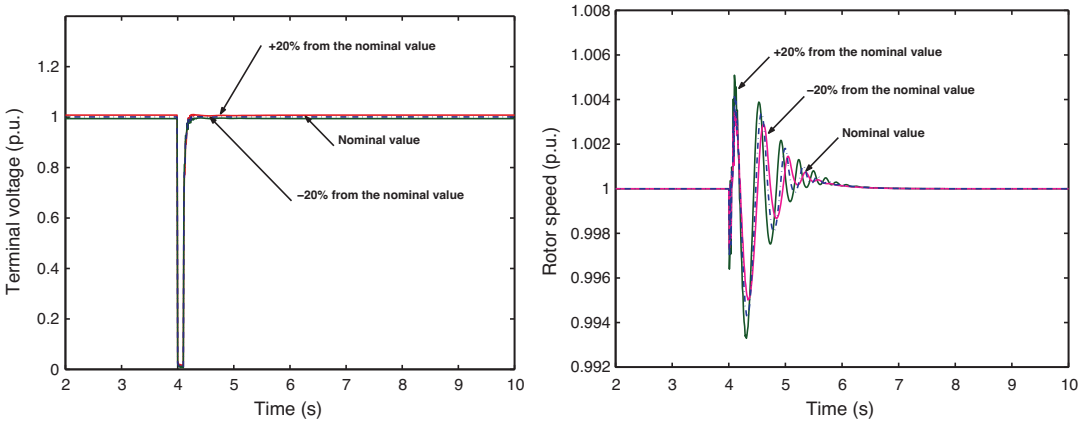

Fig. 6. Dynamic tracking performance of the proposed control scheme under parameter perturbations.

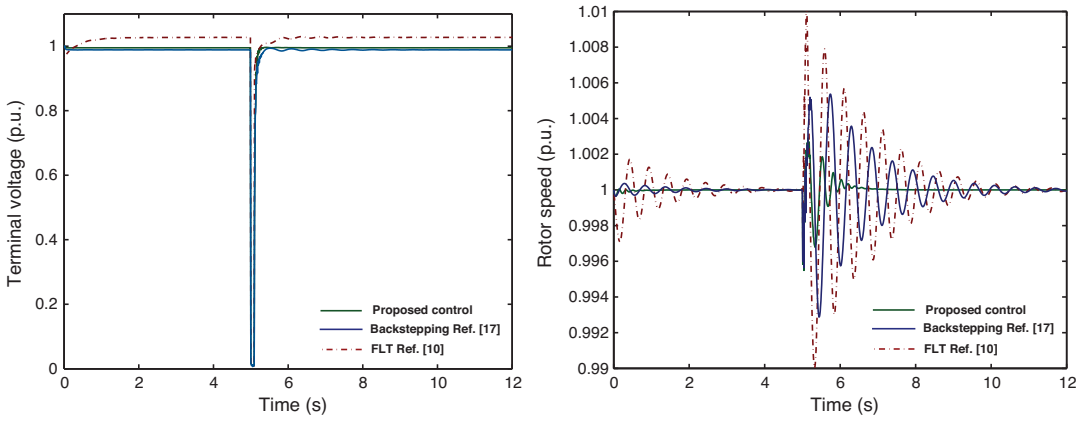

Fig. 7. Performance comparison, under −20% parameter perturbations, of the proposed control scheme and nonlinear controllers (backstepping Ref. [17] and feedback linearization technique Ref. [10]).

5. Simulation results and discussion

In order to show the validity of the mathematical analysis and, hence, to evaluate the performance of the designed nonlinear control scheme, simulation works are carried out for the Power System under severe disturbance conditions which cause significant deviation in generator loading. The performance of the nonlinear controller was tested on the complete 9th order model of SMIB power system (202 MVA, 13,7 kV), including all kinds of nonlinearities such as exciter ceilings, control signal limiters, etc. and speed regulator. The physical limits of the plant are:

$$\max|v_{fd}| = 10\,\text{p.u.}, \quad \text{and} \quad 0 \le X_e(t) \le 1$$

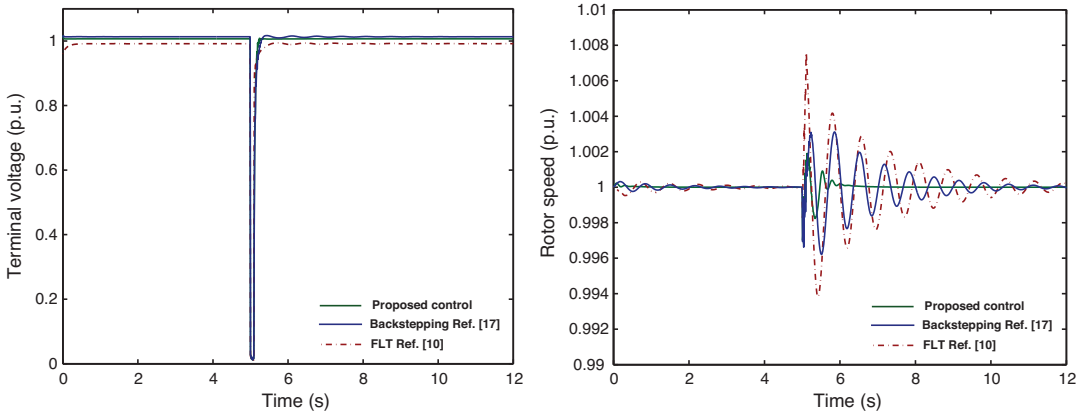

Fig. 8. Performance comparison, under +20% parameter perturbations, of the proposed control scheme and nonlinear controllers (backstepping Ref. [17] and feedback linearization technique Ref. [10]).

Table 1
Parameters of the transmission line in p.u.

Parameter	Value
L_e, inductance of the transmission line	0.4
R_e, resistance of the transmission line	0.02

Table 2
Parameters of the power synchronous generator in p.u.

Parameter	Value
R_s, stator resistance	1.096×10^{-3}
R_{fd}, field resistance	7.42×10^{-4}
R_{kd}, direct damper winding resistance	13.1×10^{-3}
R_{kq}, quadrature damper winding resistance	54×10^{-3}
L_d, direct self-inductance	1.700
L_q, quadrature self-inductances	1.640
L_{fd}, rotor self inductance	1.650
L_{kd}, direct damper winding self inductance	1.605
L_{kq}, quadrature damper winding self inductance	1.526
L_{md}, direct magnetizing inductance	1.550
L_{mq}, quadrature magnetizing inductance	1.490
V^{∞}, infinite bus voltage	1
D, damping constant	0
H, inertia constant	2.37 s

Table 3
Parameters of the steam turbine and speed governor.

Parameter	Value
T_t, time constant of the turbine	0.35 s
K_t, gain of the turbine	1
R regulation constant of the system	0.05
T_g, time constant of the speed governor	0.2 s
K_g, gain of the speed governor	1

The system configuration is presented as shown in Fig. 1. The simulation of the proposed sliding mode damper currents observer is implemented based on the scheme shown in Fig. 2. Digital simulations have been carried out using Matlab–Simulink. The parameter values used in the ensuing simulation are given in the Appendix B.

5.1. Observer based controller performance evaluation

First, we verify the stability and asymptotic tracking performance of the proposed control systems. The simulated results are given in Figs. 3 and 4. It is shown terminal voltage, rotor speed and rotor angle of the power system, respectively. The operating points considered are $P_m = 0.6$ p.u. and 0.9 p.u. The fault considered in this paper is a symmetrical three-phase short circuit, which occurs closer to the generator bus, at $t = 10$ s and removed by opening the barkers of the faulted line at $t = 10.1$ s. The results are compared with those of the linear IEEE type 1 AVR + PSS and speed regulator. As it can be seen, the proposed controller can quickly and accurately track the desired terminal voltage and rotor speed despite the different operating points.

5.2. Comparison of dynamic performances for proposed controller and non linear controllers

In order to prove the robustness of the proposed controller, the results are compared with two non linear controllers: (i) Feedback Linearization Technique (FLT) Ref. [10] and (ii) Backstepping Ref. [17]. The operating point considered is $P_m = 0.725$ p.u. The fault occurs closer to the generator bus. The simulation results are presented in Fig. 5. It can be seen that both dynamics of the terminal voltage and the rotor speed settle to their prefault values very quickly with proposed observer based controller. It is obvious that with the derived high control accuracy and stability can be achieved.

5.3. Robustness to parameters uncertainties

The variation of system parameters is considered for robustness evaluation of the proposed observer-based controller. The values of the transmission line (L_e, R_e) and the inertia constant H increased by +20% and −20% from their original values, respectively. The responses of the terminal voltage and rotor speed are shown in Fig. 6. In addition to the abrupt and permanent variation of the power system parameters a three-phase short-circuit is simulated at the terminal of the generator. Figs. 7 and 8 show the performances of the combined observer controller and the other controllers Ref. [10] and Ref. [17]. It can be seen that the designed control scheme is able to deal with the uncertainties of parameters and preserve the global stability of the system with good performances in transient and steady states.

6. Conclusion

In this paper, a new nonlinear observer–controller scheme has been developed and applied to the single machine infinite bus power system, based on the complete 7th order model of the synchronous generator. The aim of the study is to achieve both transient stability enhancement and good postfault performance of the generator terminal voltage.

The sliding mode strategy was adopted to develop a nonlinear observer of damper winding currents and nonlinear terminal voltage and rotor speed controller. The detailed derivation for the control laws has been provided. Globally exponentially stable of both the observer and control laws has been proven by applying Lyapunov stability theory.

Simulation results have confirmed that the observer-based nonlinear controller can effectively improve the transient stability and voltage regulation under large sudden fault. The combined observer–controller scheme demonstrates consistent superiority opposed to a system with linear controllers (IEEE type 1 AVR + PSS) and nonlinear controllers. It can be seen from the simulation study that the designed sliding mode observer based-controller possesses a great robustness to deal with parameter uncertainties.

Appendix A. The coefficients of the mathematical model

$$a_{11} = -(R_s + R_e)(L_{fd}L_{kd} - L_{md}^2)\omega_R D_d^{-1}, \quad a_{12} = -R_{fd}(L_{mq}L_{kd} - L_{md}^2)\omega_R D_d^{-1}, \quad a_{13} = (L_q + L_e)(L_{md}L_{kd} - L_{md}^2)\omega_R D_d^{-1}$$

$$a_{15} = -L_{mq}(L_{fd}L_{kd} - L_{md}^2)\omega_R D_d^{-1}, \quad a_{14} = R_{kd}((L_d + L_e)L_{md} - L_{md}^2)\omega_R D_d^{-1}, \quad a_{16} = -V^{\infty}((L_d + L_e)L_{kd} - L_{md}^2)\omega_R D_d^{-1}$$

$$b_1 = (L_{md}L_{kd} - L_{md}^2)\omega_R D_d^{-1}, \quad a_{21} = -(R_s + R_e)(L_{md}L_{kd} - L_{md}^2)\omega_R D_d^{-1}, \quad a_{22} = -R_{fd}((L_d + L_e)L_{kd} - L_{md}^2)\omega_R D_d^{-1}$$

$$a_{23} = (L_q + L_e)(L_{md}L_{kd} - L_{md}^2)\omega_R D_d^{-1}, \quad a_{24} = R_{kd}((L_d + L_e)L_{md} - L_{md}^2)\omega_R D_d^{-1}, \quad a_{25} = -L_{mq}(L_{md}L_{kd} - L_{md}^2)\omega_R D_d^{-1}$$

$$a_{26} = -V^{\infty}(L_{md}L_{kd} - L_{md}^2)\omega_R D_d^{-1}, \quad b_2 = ((L_d + L_{fd})L_{kd} - L_{md}^2)\omega_R D_d^{-1}, \quad a_{31} = -(L_d + L_e)L_{kq}\omega_R D_q^{-1}$$

$$a_{32} = L_{md}L_{kq}\omega_R D_q^{-1}, \quad a_{33} = -(R_s + R_e)L_{kq}\omega_R D_q^{-1}, \quad a_{34} = L_{md}L_{kq}\omega_R D_q^{-1}, \quad a_{35} = -L_{mq}.R_{kq}\omega_R D_q^{-1}, \quad a_{36} = V^{\infty}L_{kq}\omega_R D_q^{-1}$$

$$a_{41} = -(R_s + R_e)(L_{fd}L_{md} - L_{md}^2)\omega_R D_d^{-1}, \quad a_{42} = R_{fd}((L_d + L_e)L_{md} - L_{md}^2)\omega_R D_d^{-1}, \quad a_{45} = -L_{md}(L_{mq}.L_{fd} - L_{md}^2)\omega_R D_d^{-1}$$

$$a_{43} = (L_q + L_e)(L_{md}L_d - L_{md}^2)\omega_R D_d^{-1}, \quad a_{44} = -R_{kd}((L_d + L_e)L_{fd} - L_{md}^2)\omega_R D_d^{-1}, \quad a_{46} = -V^{\infty}(L_{md}.L_{fd} + L_{md}^2)\omega_R D_d^{-1}$$

$$b_3 = ((L_d + L_e)L_{md} - L_{md}^2)\omega_R D_d^{-1}, \quad a_{51} = -(L_d + L_e)L_{mq}\omega_R D_q^{-1}, \quad a_{52} = L_{md}L_{mq}\omega_R D_q^{-1}, \quad a_{53} = -(R_s + R_e)L_{mq}\omega_R D_q^{-1}$$

$$a_{54} = L_{md}L_{mq}\omega_R D_q^{-1}, \quad a_{55} = -R_{kq}(L_q + L_e)\omega_R D_q^{-1}, \quad a_{56} = -V^{\infty}L_{mq}\omega_R D_d^{-1}, \quad a_{61} = -D(2H)^{-1}, a_{62} = (2H)^{-1}$$

$$a_{81} = -(T_m)^{-1}, \quad a_{82} = K_m(T_m)^{-1}, \quad a_{91} = -(T_g)^{-1}, \quad a_{92} = -K_g(T_g R\omega_R)^{-1}, \quad b_4 = K_g(T_g)^{-1}, \quad c_{11} = R_e + a_{11}L_e\omega_R^{-1}$$

$$c_{12} = a_{12}L_e\omega_R^{-1}, \quad c_{13} = L_e(a_{13}\omega_R^{-1} - 1), \quad c_{14} = a_{14}L_e\omega_R^{-1}, \quad c_{15} = a_{15}L_e\omega_R^{-1}, \quad c_{16} = V^{\infty} + a_{16}L_e\omega_R^{-1}, \quad c_{17} = b_1L_e\omega_R^{-1}$$

$$c_{21} = L_e + a_{31}L_e\omega_R^{-1}, \quad c_{22} = a_{32}L_e\omega_R^{-1}, \quad c_{23} = a_{33}L_e\omega_R^{-1} + R_e, \quad c_{24} = a_{34}L_e\omega_R^{-1}, \quad c_{25} = a_{35}L_e\omega_R^{-1}, \quad c_{26} = V^{\infty} + a_{36}L_e\omega_R^{-1}$$

here we have denoted

$$D_d = (L_d + L_e)L_{fd}L_{kd} - L_{md}^2(L_d + L_{fd} + L_{kd}) + 2L_{md}^3, \quad D_q = (L_q + L_e)L_{kq} - L_{mq}^2$$

Appendix B. The parameters of the system are as follows [24,25] (Tables 1–3)

References

[1] Y. Guo, D.J. Hill, Y. Wang, Global transient stability and voltage regulation for power systems, IEEE Transactions on Power Systems 16 (2001) 678–688.
[2] C. Zhu, R. Zhou, Y. Wang, A new nonlinear voltage controller for power systems, International Journal of Electrical Power and Energy Systems 19 (1996) 19–27.
[3] Z. Xi, G. Feng, D. Cheng, Q. Lu, Nonlinear decentralized saturated controller design for power systems, IEEE Transactions on Control Systems Technology 11 (2003) 509–518.
[4] W. Lin, T. Shen, Robust passivity and feedback design for minimum-phase nonlinear systems with structural un certainty, Automatica 35 (1999) 35–48.
[5] A. Isidori, Nonlinear Control System, Springer Verlag, Berlin, 1989.
[6] Y. Wang, D.J. Hill, R.H. Middleton, L. Gao, Transient stability enhancement and voltage regulation of power systems, IEEE Transactions on Power Systems 2 (1993) 620–628.
[7] E. De Tuglie, S. Marcello Iannone, F. Torelli, Feedback-linearization and feedback–feedforward decentralized control for multimachine power system, Electric Power Systems Research 78 (2008) 382–391.
[8] C.A. King, J.W. Chapman, M.D. Ilic, Feedback linearizing excitation control on a full-scale power system model, IEEE Transactions on Power Systems 2 (1994) 1102–1110.
[9] S. Jain, F. Khorrami, B. Fardanesh, Adaptive nonlinear excitation control of power system with unknown interconnections, IEEE Transactions on Control Systems Technology 4 (1994) 436–447.
[10] O. Akhrif, F.A. Okou, L.A. Dessaint, R. Champagne, Application of mulitivariable feedback linearization scheme for rotor angle stability and voltage regulation of power systems, IEEE Transactions on Power Systems 4 (1999) 620–628.
[11] L. Yan-Hong, L. Chun-Wen, W. Yu-Zhen, Decentralized excitation control of multi-machine multi-load power systems using Hamiltonian function method, Acta Automatica Sinica 35 (2009) 921–925.
[12] T. Shen, S. Mei, Q. Lu, W. Hu, K. Tamura, Adaptive nonlinear excitation control with L2 disturbance attenuation for power systems, Automatica 39 (2003) 81–90.
[13] A.Y. Pogromsky, A.L. Fradkov, D.J. Hill, Passivity based damping of power system oscillations, in: Proceedings of the IEEE CDC, Kobe, Japan, 1996.
[14] R. Ortega, A. Stankovic, P.A. Stefanov, Passivation approach to power systems stabilization, in: Proceedings of the IFAC NOLCOS, Enshede, Netherlands, 1998.
[15] P. Hoang, K. Tomsovic, Design and analysis of an adaptive fuzzy power system stabilizer, in: Proceedings of the IEEE PES Winter Meeting, 1996.
[16] J. Wook Park, G. Ronald Harley, K. Ganesh Venayagamoorthy, Decentralized optimal neuro-controllers for generation and transmission devices in an electric power network, Engineering Applications of Artificial Intelligence 18 (2005) 37–46.
[17] M. Ouassaid, A. Nejmi, M. Cherkaoui, M. Maaroufi, A nonlinear backstepping controller for power systems terminal voltage and rotor speed controls, International Review of Automatic Control 3 (2008) 355–363.
[18] A. Karimi, A. Feliachi, Decentralized adaptive backstepping control of electric power systems, International Electric Power Systems Research 78 (2008) 484–493.
[19] P. Kundur, Power System Stability and Control, MacGraw-Hill, 1994.
[20] M.S. Ghazizadeh, F.M. Hughs, A generator transfer function regulator for improved excitation control, IEEE Transactions on Power Systems 13 (1998) 437–441.
[21] Adil., A. Ghandakly, A.M. Farhoud, A parametrically optimized self tuning regulator for power system stabilizers, IEEE Transactions on Power Systems 7 (1992) 1245–1250.
[22] Q. Zhao, J. Jiang, Robust controller design for generator excitation systems, IEEE Transactions on Energy Conversion 10 (1995) 201–207.
[23] V.I. Utkin, J. Guldner, J. Shi, Sliding Mode Control in Electromechanical Systems, Taylor and Francis, London, 1999.
[24] P.M. Anderson, A.A. Fouad, Power System Control and Stability, IEEE Press, 1994.
[25] D.J. Hill, Y. Wang, Nonlinear decentralized control of large scale power systems, Automatica 36 (2000) 1275–1289.
[26] F.P. de Mello, Measurement of synchronous machine rotor angle from analysis of zero sequence harmonic components of machine terminal voltage, IEEE Transactions on Power Delivery 9 (1994) 1770–1777.
[27] V.I. Utkin, Sliding mode control design principles and applications to electric drives, IEEE Transactions on Industrial Electronics 40 (1993) 23–36.